Thermoelectric amplification of acoustic waves observed in Ni using optical-beam-deflection detection

N. A. S. Rodrigues
Instituto de Estudos Avançados, Centro Técnico Aeroespacial, Caixa Postal 6044, 12 201 São José dos Campos, São Paulo, Brazil

L. C. M. Miranda
Laboratório Associado de Sensores e Materiais, Instituto de Pesquisas Espaciais, Caixa Postal 515, 12 201 São José dos Campos, São Paulo, Brazil
(Received 13 March 1990)

The onset of the spectrally resolved acoustic-wave instability in Ni in the presence of a temperature gradient is observed. The detection technique used is the noncontact optical-probe-beam deflection.

I. INTRODUCTION

In previous papers[1,2] we have reported on the observation of acoustic wave instabilities in a Ni sample due to the temperature gradient induced by intense CO_2 laser pulses. To our knowledge, this was the first experimental evidence of the so-called thermoelectric amplification of acoustic waves.[3–6] The latter phenomenon is one of several giving rise to acoustic waves in semiconductors and metals. The best known of these mechanisms is the amplification of acoustic waves in an external dc electric field.[7,8] The basic idea of the thermoelectric amplification of acoustic waves may be summarized as follows.[3–6] Under the action of a temperature gradient, a semiconductor or a metal develops an electric current such that the carrier drift velocity v_d is given by[4,5]

$$v_d = \frac{\chi \tau k_B |\nabla T|}{m} , \tag{1.1}$$

where τ is the carrier relaxation time, ∇T is the temperature gradient in the sample, and χ is a factor which depends on the electron scattering mechanism and whether the electrons are degenerated or not.[5] Equation (1.1) means that there is a thermoelectric field applied to the sample, which, in turn, causes the space charge to drift; if the drift velocity is greater than the sound velocity v_s in the sample, the bunches of carriers will emit phonons, in complete analogy with the acoustoelectric effect.

In Refs. 1 and 2 the thermoelectric amplification was demonstrated using a CO_2 transversely excited atmospheric (TEA) laser to establish the temperature gradient. The sample used was 500-μm-thick Ni sample so that the absorbed radiation would take place very close to the irradiates surface (surface absorption). To enhance the radiation absorption the sample surface on which the laser beam impinged was previously oxidized. The acoustic waves generated by the laser pulses were detected by means of a 28-μm-thick poly(vinyl difluoride) (PVDF) piezoelectric film attached to the opposite nonilluminated surface of the sample. The thermoelectric amplification was evidenced by the exponential growth of the transducer signal as a function of the laser pulse energy above the threshold pulse energy determined from the condition $v_d \geq v_s$. These results were, however, broadband integrated results in the sense that all the acoustic waves that were reaching the detector contributed to the signal. In this paper we present a spectral analysis of the thermoelectric amplification of acoustic waves under the same experimental conditions as those of Refs. 1 and 2. This was done by taking the Fourier transform of the detected signal and monitoring the behavior of its components as a function of the laser pulse energy. In carrying out this study we have used a different detection technique than that used in Refs. 1 and 2. The technique used was the optical probe beam deflection (mirage effect). This noncontact technique has been extensively used in photothermal studies.[9–12] It is based on the fact that an optical probe beam, say, from a He-Ne laser, propagating in the medium surrounding the sample will be deflected as it crosses the region adjacent to the sample surface due to the refractive index gradient induced in the medium by coming from the sample.

In Sec. II we present a theoretical background of the thermoelectric amplification of acoustic waves as well as of the detection scheme. The experimental apparatus and procedures are presented in Sec. III, whereas in Sec. IV the results and the discussion of our data are given.

II. THEORY

Consider an electron-phonon system subjected to a temperature gradient along the x direction. The equation describing the propagation of elastic waves of frequency ω along the x direction is

$$\rho \frac{\partial^2 u}{\partial t^2} = C \frac{\partial^2 u}{\partial x^2} - \beta \frac{\partial E}{\partial x} , \tag{2.1}$$

where u is the lattice displacement, ρ is the density of the material, C is elastic constant, β is the coupling constant for the electron-lattice interaction, and E is the electric

field due to the acoustic wave. To solve Eq. (2.1) for u, we must express E in terms of the lattice displacement. The equations used in this connection are the modified Poisson equation obtained from

$$\frac{\partial D}{\partial x} = -en_s \ , \tag{2.2}$$

where D is the electric displacement, given by

$$D = \epsilon E + \beta \frac{\partial u}{\partial x} \ , \tag{2.3}$$

and the equation of charge continuity

$$\frac{\partial J}{\partial x} = e\frac{\partial n_s}{\partial t} \ . \tag{2.4}$$

In Eqs. (2.2)–(2.4), n_s is the space-charge density, J is the current density, and ϵ is the dielectric constant at constant strain.

For an electron gas in a crystal in the presence of the electric field of the acoustic wave and subjected to gradients in electrochemical potential and temperature, the general expression for the current density is[13]

$$J = \sigma E + eD_c \frac{\partial n}{\partial x} + n\mu \frac{Q}{T}\frac{\partial T}{\partial x} \ , \tag{2.5}$$

where μ is the carrier mobility, $\sigma = ne\mu$ is the electrical conductivity, D_c is the carrier diffusion coefficient, and $Q = \chi k_B T$ is the heat of the electron transport. The second term in Eq. (2.5) is due to carrier diffusion caused by the concentration gradient accompanying a temperature gradient, and the last term, due to the temperature gradient, represents the thermoelectric field. For a nondegenerate electron gas, D_c reduces to the well-known Einstein relation, namely, $D_c = k_B T\mu/e$, whereas for a degenerate electron gas, $D_c = (\frac{2}{3})\mu\varepsilon_F/e$. The value of χ (and therefore of Q) depends on the dominant electron-phonon scattering mechanism as well as whether the electron gas is degenerate or not; for example, for a degenerate electron gas, $\chi = \pi^2 k_B T/3\varepsilon_F$. The carrier density is $n = n_0 + n_s$, where n_0 is the equilibrium density and n_s is the space-charge density. Keeping only first-order terms, one gets from Eqs. (2.2) and (2.5)

$$-\frac{\partial^2 D}{\partial t \partial x} = \sigma\frac{\partial E}{\partial x} + eD_c\frac{\partial^2 n_s}{\partial x^2} + \chi k_B \mu \frac{\partial T}{\partial x}\frac{\partial n_s}{\partial x} \ . \tag{2.6}$$

Assuming that u, E, n_s, and D vary harmonically as $\exp[j(kx - \omega t)]$, where k is the wave vector of the acoustic wave, Eqs. (2.2), (2.3), and (2.6) give us a relation between E and u. Using this relation into the wave Eq. (2.1) leads to the following dispersion relation:

$$\frac{\beta^2}{\epsilon\rho}\left[\frac{k^2}{\omega^2 - k^2 v_s^2}\right] = 1 + \frac{j\sigma/\epsilon}{\omega - kv_d + jk^2 D_c} \ , \tag{2.7}$$

where $v_d = -(\chi k_B \tau/m)\partial T/\partial x$ is the drift velocity due to the temperature gradient, $v_s = (C/\rho)^{1/2}$ is the sound velocity, and $j \equiv \sqrt{-1}$. To find the attenuation coefficient α for the acoustic wave, we write $k = k_0 + j\alpha$, where $k_0 = \omega/v_s$. Substituting this expression for k in Eq. (2.7) and solving it one finds the renormalized sound velocity and the attenuation coefficient. Let us define the following parameter $\gamma = 1 - v_d/v_s$ as a measure of the ratio the drift velocity to the sound velocity, the dielectric laxation frequency $\omega_c = \sigma/\epsilon$, and the electromechan coupling coefficient $K = (\beta^2/\epsilon C)^{1/2}$. Noting that long-wavelength acoustic waves we can neglect diffusion term on the right-hand side of Eq. (2.7), making the approximation that the attenuation is sn $(k_0 \ll |\alpha|)$, one gets from the solution to Eq. (2.7)

$$\alpha = \gamma\frac{K^2}{2}\frac{\omega_c}{v_s}\frac{1}{(\gamma^2 + \omega^2/\omega^2)} \ . \tag{2}$$

When α is negative, the acoustic waves grow in amp tude instead of diminishing. It follows from Eq. (2.8) t α becomes negative when γ is negative, or rather, wh the drift velocity exceeds the sound velocity, for acous waves propagating in the direction of the heat flux.

To actually observe the thermoelectric amplificati using laser-produced temperature gradient, the la pulse energy E_p and the pulse duration τ_p should chosen such that (i) the heat deposited at the sample s face does not diffuse appreciably during the pulse du tion, and (ii) the optical penetration depth β_0^{-1} is mu smaller than the sample length l. We define the followi parameters: λ, the thermal conductivity of the sample; the specific heat; $\alpha_t = \lambda/\rho c$, the thermal diffusivi $\tau_d = \pi l^2/\alpha_t$, the thermal diffusion time in the sample; the optical absorption coefficient. The second conditio $\beta_0 l \ll 1$, is easily satisfied for a Ni sample irradiated the long-wavelength radiation of a CO_2 laser. Conditi (ii), in turn, requires the thermal diffusion time in t sample to be much greater than the pulse duration, $l \ll (\alpha_t \tau_p/\pi)^{1/2}$. Using the values of α_t for Ni, given Table I, the thermal diffusion length for a pulse durati of 100 ns turns out to be 0.86 μm. This means that for 500-μm-thick Ni sample we can produce a well-defin temperature gradient using CO_2 pulses of 100-ns dur tion. Finally, the condition $v_d \geq v_s$ for the onset of t thermoelectric amplification imposes a threshold on t laser pulse energy E_p. In terms of the laser pulse energ the temperature rise and the temperature gradient at t sample surface is given by[14]

$$\Delta T = \frac{2\eta E_p}{A\rho c(\pi\alpha_t)^{1/2}} \tag{2.}$$

and

TABLE I. Values of the physical parameters of Ni used the text. The literature values taken from Ref. 21.

Physical parameter	Literature valu
Density (g/cm^3)	8.91
Specific heat (J/g K)	0.44
Thermal conductivity (W/cm K)	0.9
Thermal diffusivity (cm^2/s)	0.2
Electrical conductivity (s^{-1})	1.1×10^{17}
Carrier concentration (cm^{-3})	5.4×10^{22}
Sound velocity (cm/s)	3×10^5

$$|\nabla T| = \frac{\sqrt{2}}{2} \frac{\eta E_p}{A \rho c \alpha_t \tau_p} , \tag{2.10}$$

where η is the light-into-heat conversion efficiency and A is the illuminated area. To get Eqs. (2.9) and (2.10), the heat conduction equation was solved for the uniform heating over the surface bounding a semi-infinite sample, supposing a rectangular laser pulse with energy E_p and duration T_p. Equation (2.10) is equivalent to a slab $2\sqrt{2}l_d$ thick with a temperature difference between surfaces of ΔT, where l_d is the thermal diffusion length. Supposing that the main electron scattering mechanism is due to the ions, where the electron relaxation is given by $\tau = \tau_0 (T/T_0)^{3/2}$, and integrating Eq. (1.1) from 0 to $2\sqrt{2}l_d$, we obtain the threshold surface temparture rise for thermoelectric amplification:

$$\Delta T_{\text{th}} = T_0 \left[\left[1 + \frac{21\sqrt{2} m v_s \varepsilon_F l_d}{\pi^2 k_B^2 \tau_0 T_0^2} \right]^{2/7} - 1 \right] . \tag{2.11}$$

Comparing with Eq. (2.10), we obtain the threshold laser pulse energy

$$E_{p,\text{th}} = \frac{\rho c A (\pi \alpha_t \tau_p)^{1/2} T_0}{2\eta} \times \left[\left[1 + \frac{21\sqrt{2} m v_s \varepsilon_F l_d}{\pi^2 k_B^2 \tau_0 T_0^2} \right]^{2/7} - 1 \right] . \tag{2.12}$$

Substituting the Ni constants shown in Table I, we have

$$E_{p,\text{th}} = 4.66 \times 10^6 \frac{A \tau_p^{1/2}}{\eta} \times [(1 + 1.75 \times 10^6 \tau_p^{1/2})^{2/7} - 1] . \tag{2.13}$$

Finally, we briefly outline the theory of the detection scheme used. Consider a He-Ne laser probe beam propagating in the medium (e.g., air, water, etc.) surrounding the back nonilluminated surface of our sample. The probe beam propagates parallel to the sample surface at a distance x_0 from it, as indicated in Fig. 1. The effect of the laser pulses at $x = -l$ is twofold. First, the temperature rise ΔT at $x = -l$ generates acoustic waves[15,16] as a result of thermal expansion (i.e., $u \sim \alpha_t \Delta T$). Parallel to this, the temperature gradient set in the sample may amplify these acoustic waves due to the electron-phonon interaction, provided that Eq. (2.12) is satisfied. We thus expect pulses of acoustic (fast) and thermal (slow) waves to be propagating down the sample. For a 500-μm-thick Ni sample, the transit time for the acoustic waves is typically of the order of 0.2 μs, whereas the thermal diffusion time is roughly 34 ms. These waves are transmitted into the surrounding medium as they reach the interface at $x = 0$, thereby producing pressure and temperature gradients in the fluid. Thus, in turn, implies that the refractive index of the surrounding fluid, n_f, will exhibit a gradient given by

$$\frac{\partial n_f}{\partial x} = \frac{\partial n_f}{\partial p} \frac{\partial p}{\partial x} + \frac{\partial n_f}{\partial T} \frac{\partial T}{\partial x} , \tag{2.14}$$

where p and T are the pressure and the temperature in the fluid, respectively. The probe beam passing though a region where the refractive index varies in space and time experiences a deflection. For small probe deflections geometrics optics[10,17] tells us that the deflection angle θ is given by (c.f., Fig. 1)

$$\theta = \frac{L}{n_{f0}} \left[\frac{\partial n_f}{\partial x} \right]_{x = x_0} , \tag{2.15}$$

where n_{f0} is the refractive index of the fluid at ambient pressure and temperature and L is the length of the interaction region between the probe beam and the pressure gradient, of the order of the sample width.

The detection of refractive index variation caused by acoustic waves is not new; for example it has been reported by Lucas and Biquard[18] and by Davidson and Emmony.[19] More recently, Sullivan and Tam[20] have used it to detect photoacoustic pressure pulses. The detection of the probe beam deflection is usually made either using a position sensor or with a knife edge, which blocks half of the probe beam diameter, followed by a photocell. In either case, the signal at the detector is proportional to the pressure gradient at $x = x_0$ or, alternatively, proportional to $-\rho \partial^2 u / \partial t^2$. In other words, the detected signal will be proportional to the acoustic wave amplitude at $x = x_0$. Thus, as long as we have no amplification the signal is expected to vary linearly with the driving pulse energy E_p (i.e., $u \sim \alpha_t \Delta T$), whereas when the amplification sets in it is expected to grow exponentially with v_d, and, therefore, to E_p.

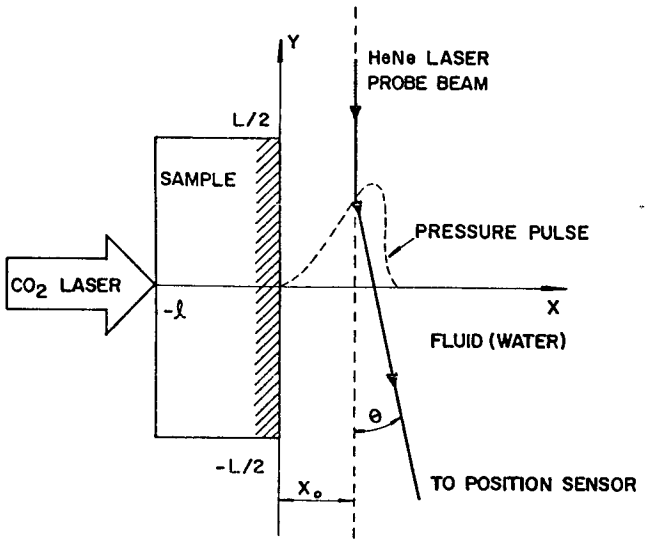

FIG. 1. Probe beam deflection due to the pressure pulse generated by the laser pulse on the sample surface.

III. EXPERIMENTAL

In Fig. 2 we show our experimental arrangement. It consists of focusing the pulses from a CO_2 TEA laser on one face of a 500-μm-thick Ni sample by means of a Ge lens producing a spot size of 0.6-mm diameter. The laser pulse energy was measured by means of a pyroelectric energy meter (Molectron J3-05). The sample was posi-

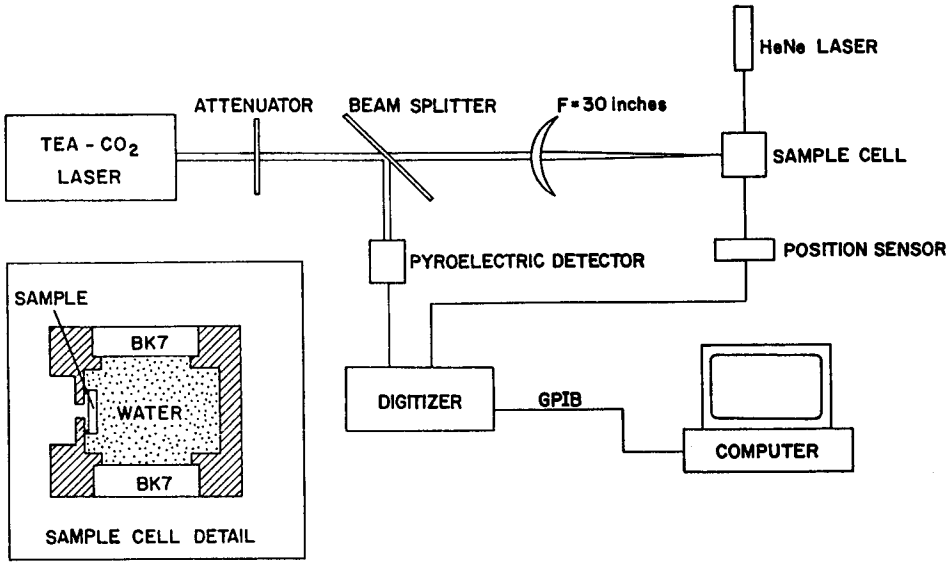

FIG. 2. Experimental setup. The inset shows sample-cell details.

tioned in such a way as to close an aluminum cell which was previously filled with water as shown in the inset of Fig. 2. This cell had two BK-7 optical glass windows to allow for the tangential positioning of the He-He laser probe beam near the nonilluminated sample surface. The probe been deflections were monitored using a position sensor placed at a suitable distance outside the cell. The use of water in a closed cell was dictated by two factors, namely, to enhance the acoustic impedance matching between the sample and the transducing medium, and by the fact that $\partial n/\partial p$ for liquids is greater than for gases. The output signal from the position sensor, after being amplified, was fed into a programmable digitizer (Tektronix 7D-20) attached to an oscilloscope. The CO_2 laser pulse energy was varied by means of a Mylar attenuator of variable thickness. Each data point reported in what follows corresponds to a average over 16 pulses at a repetition rate of 1 Hz.

We measured the reflectivity of the oxidized Ni sar to be about 60%. If the complete light-into-heat con sion for the nonreflected laser pulses is supposed, we tain $\eta=0.4$.

IV. RESULTS AND DISCUSSION

In Fig. 3 we show the output probe beam signal function of time for the case of irradiation with a 27.1 pulse. At longer times, of the order of several tens n second broad single pulse is also observed. This sec pulse is the so-called thermal pulse coming from the diffusion. Apart from the residual vibrations of the c cal bench and the fluctuation in the He-Ne laser inter and of the refractive index of the air, the main sourc noise came from the CO_2 laser itself. By blocking CO_2 laser pulses so that they were not reaching the s ple, we have verified that the laser noise persists onl to 10 μs.

To monitor the behavior of the acoustic waves

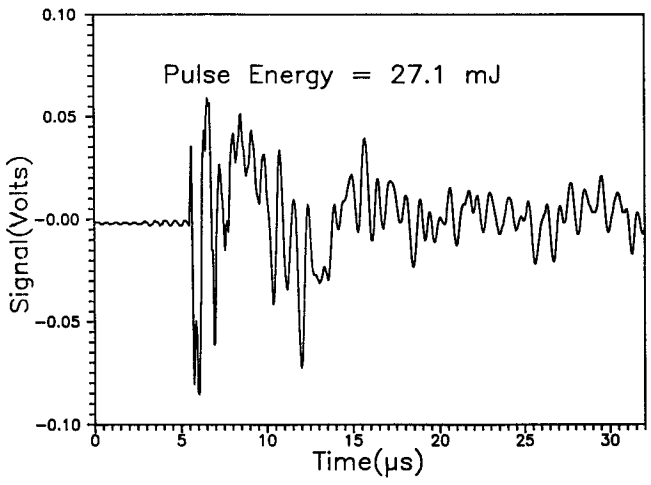

FIG. 3. Typical position sensor electric signal for a 27.1-mJ laser pulse striking the sample surface.

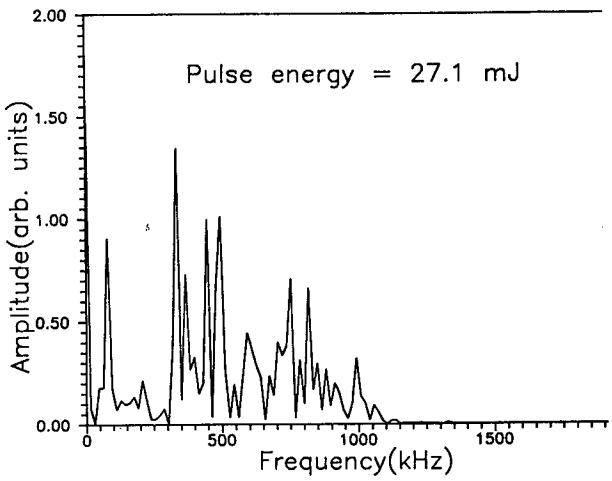

FIG. 4. Frequency spectrum for the signal shown in Fig.

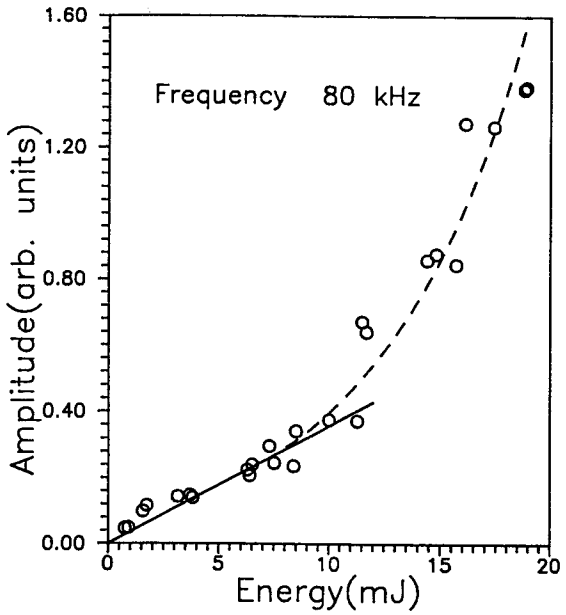

FIG. 5. 80-kHz component elastic wave amplitude against pulse energy for 320-ns laser pulse duration. The experimental data up to 5 mJ are best fitted by a straight line (solid) and, for higher energies, the best fit is given by an exponential line (dashed).

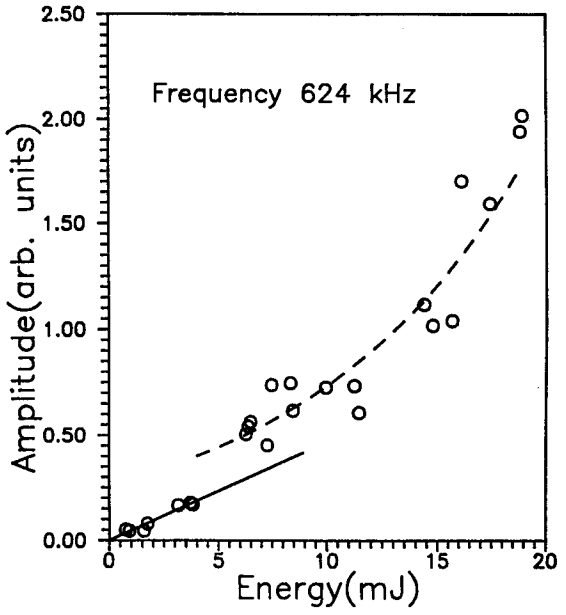

FIG. 7. 628-kHz component elastic wave amplitude against pulse energy for the same conditions as in Fig. 5.

given frequency we performed a spectral analysis. This was done by taking the Fourier transform of the deflection signal and monitoring the behavior of the amplitude of each component as a function of the laser pulse energy. In Fig. 4 we show the Fourier spectrum for the irradiation with a 27.1-mJ CO_2 laser pulse. This spectrum was obtained from the output signal shown in Fig. 3, neglecting the region where we still had the laser noise; i.e., we just considered the signal output for $t > 10\ \mu s$. In Figs. 5–7, we show the dependence on the CO_2 laser pulse energy of the 80-, 208-, and 624-kHz Fourier components, respectively, when the sample was illuminated by 320-ns duration laser pulses. The solid and dashed lines in those figures correspond to the best fitting of our data to power law and exponential curves, respectively. Up to a pulse energy of roughly 5 mJ the data in Figs. 5–7 are best fitted by a curve varying linearly with E_p. Above 5 mJ the data is best fitted by an exponential curve. This transition is more clearly exhibited in Fig. 8, in which we present a semilogarithmic plot of the modulus of the 624-kHz Fourier component as a function of the laser pulse energy. This value of the pulse energy should be compared with the predict one by Eq. (2.14). Taking $A = 1.51 \times 10^{-3}$ cm^2, $\tau_p = 320$ ns, and $\eta = 0.4$, we

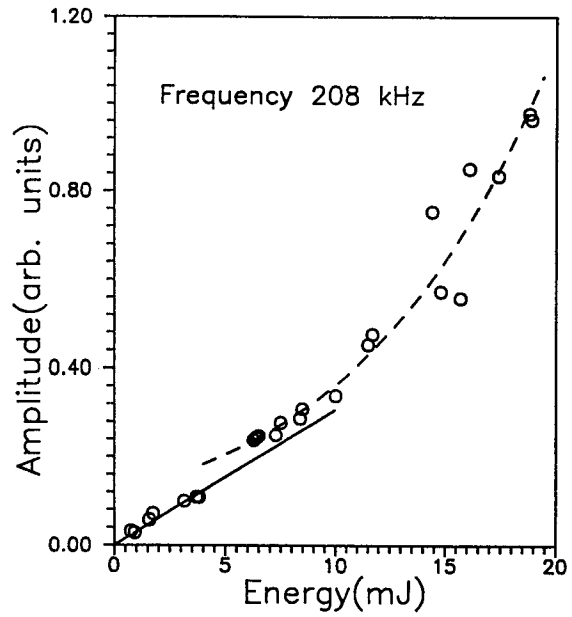

FIG. 6. 208-kHz component elastic wave amplitude against pulse energy for the same conditions as in Fig. 5.

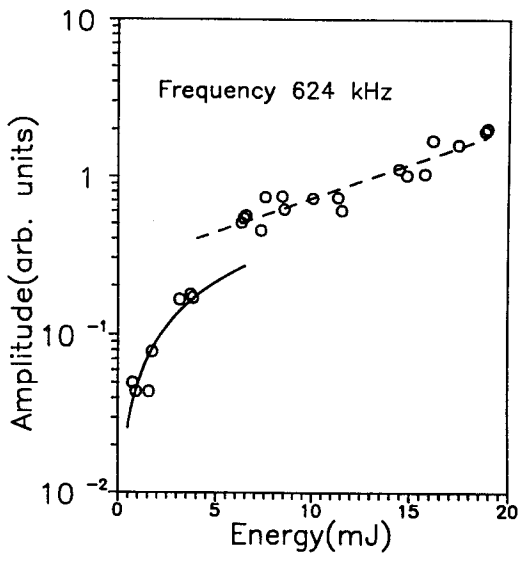

FIG. 8. Semilogarithmic plot of the same data shown in Fig. 7.

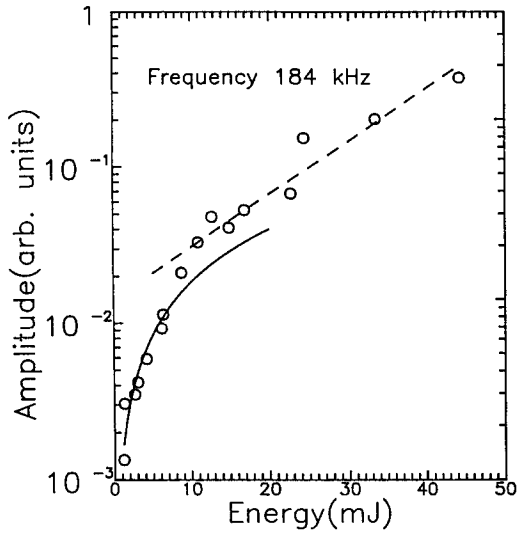

FIG. 9. 184-kHz component elastic wave amplitude against pulse energy for 970-ns laser pulse duration. The experimental data up to 10 mJ are best fitted by a straight line (solid) and, for higher energies, the best fit is given by an exponential line (dashed).

obtain the threshold laser energy pulse to be 6.1 mJ, which is in good agreement with the experimental one. These results confirm the previously reported ones[1,2] for the thermoelectric amplification obtained for an integrated (over the acoustic wave frequencies) signal. Furthermore, the pulse energy at which the transition from the linear region into the instability (exponential) region took place (i.e., 5 mJ) is the same in the present spectrally resolved case as in the integrated signal experiment. The reason for this is that the threshold condition for the thermoelectric amplification to set in is independence of the acoustic wave frequency.

In Fig. 9 we show the experimental data for a 970-ns-duration laser pulse for the 184-kHz Fourier component. Up to a pulse energy of roughly 10 mJ, our data are best fitted by a curve varying linearly with E_p, while for those above this value the best fitting is given by an exponential. The theoretical predicted threshold energy value for a 970-ns laser pulse is 12.8 mJ, and again the agreement is very good.

We believe these results, together with the ones previously reported using a different detection technique, are strong evidence of the onset of thermoelectric amplification.

[1]N. A. S. Rodrigues, C. C. Ghizoni, and L. C. M. Miranda, J. Appl. Phys. **60**, 1528 (1986).
[2]N. A. S. Rodrigues, C. C. Ghizoni, and L. C. M. Miranda, Solid State Commun. **60**, 323 (1986).
[3]V. L. Bonch-Bruyevich and Yu. V. Gulyayev, Radiotekh. Elektron. **8**, 1179 (1963).
[4]S. Sharma and S. P. Singh, J. Appl. Phys. **45**, 4656 (1974).
[5]E. M. Epshtein, Fiz. Tekh. Poluprovodn. **9**, 1584 (1975) [Sov. Phys.—Semicond. **9**, 1043 (1976)].
[6]M. A. Tenan, A. Marotta, and L. C. M. Miranda, Appl. Phys. Lett. **35**, 321 (1979).
[7]A. R. Hutson, J. H. McFee, and D. L. White, Phys. Rev. Lett. **7**, 237 (1961).
[8]H. N. Spector, in *Solid State Physics*, edited by F. Seitz and D. Turnbull (Academic, New York, 1966), Vol. 19, p. 291.
[9]A. C. Boccara, D. Fournier, and J. Badoz, Appl. Phys. Lett. **36**, 130 (1980).
[10]J. C. Murphy and L. C. Aamondt, J. Appl. Phys. **51**, 4580 (1980).
[11]W. D. Jackson, N. M. Amer, A. C. Boccara, and D. Fournier, Appl. Opt. **20**, 1331 (1980).
[12]A. Mandelis, J. Appl. Phys. **54**, 3404 (1983).
[13]A. Haug, in *Theoretical Solid State Physics* (Pergamon, Oxford, 1972), Vol. 12, p. 109; see also J. Tauc, in *Photo- and-Thermo-Electric Effects in Semiconductors* (Pergamon, Oxford, 1962), p. 83.
[14]W. W. Duley, in *CO_2 Lasers: Effects and Applications* (Academic, New York, 1976), p. 139.
[15]R. M. White, J. Appl. Phys. **34**, 3559 (1963).
[16]R. J. von Gutfeld and R. L. Melcher, Appl. Phys. Lett. **33**, 257 (1977).
[17]M. Born and E. Wolf, in *Principles of Optics* (Pergamon, Oxford, 1975), p. 1562.
[18]R. Lucas and P. Biquard, J. Phys. Radium **3**, 464 (1932).
[19]G. P. Davidson and D. C. Emmony, J. Phys. E **13**, 92 (1980).
[20]B. Sullivan and A. C. Tam, J. Acoust. Soc. Am. **75**, 437 (1984).
[21]*CRC Handbook of Chemistry and Physics*, 65th ed., edited by R. C. Weast (CRC, Boca Raton, 1984).